

AD-757 096

SUBMERSIBLE MANEUVERING

C. K. Taft

New Hampshire University

Prepared for:

Office of Naval Research
Advanced Research Projects Agency

1 February 1973

DISTRIBUTED BY:

NTIS

National Technical Information Service
U. S. DEPARTMENT OF COMMERCE
5285 Port Royal Road, Springfield Va. 22151

AD 757096

TECHNICAL REPORT

SUBMERSIBLE MANEUVERING

September 1, 1972 - February 1, 1973

Sponsored by Advanced Research Projects Agency

ARPA Order No. 1958/9-27-71

Contract No. N00014-67-A-0158-0006

Dr. C. K. Taft, Principal Investigator
603-865-5074

University of New Hampshire

February 1, 1972 Contract Effect Date
January 30, 1972, Contract Expiration Date

Scientific Officer - Program Director
Ocean Technology Programs, Ocean Science and
Technology Division, O N R
800 N. Quincy Street
Arlington, VA 22217

D D C
RECEIVED
MAR 19 1973
B

The views and conclusions contained in this document are those of the authors and should not be interpreted as necessarily representing the official policies, either expressed or implied of the Advanced Research Projects Agency or the U.S. Government.

Amount of Contract \$65,112.00

Form Approved Budget Bureau No. 22-R0293

Reproduced by
NATIONAL TECHNICAL
INFORMATION SERVICE
U S Department of Commerce
Springfield VA 22151

DISTRIBUTION STATEMENT A
Approved for public release
Distribution Unlimited

SUMMARY

This report summarizes the work completed on this project during the last six months. A test facility which allows shroud shape ahead and behind the propeller to be varied easily has been constructed. In addition, several shroud shapes were tested in order to determine the sensitivity of shroud performance to exit angle and internal shroud shape at zero forward velocity. As a result of these tests, two stable states have been shown to exist for the wake steering shroud-propeller system. In order for the shroud to perform reliably in the wake steering mode, it is necessary for the wake to be completely attached to the shroud whenever a port is closed, and completely separated downstream from a port when that port is open. Thus, the shroud must operate in two stable states as determined by the control port condition. A third state was detected during the tests in which the wake would not become reattached to the shroud's inner surface when a control port was opened and then closed. This kind of behavior would obviously be intolerable in any wake steering shroud design using our present control concept. While it may be possible, however, to modify our control concept and still operate in this third state, this alternative is not being pursued at the moment.

Tests are continuing with a series of shrouds which have an internal shape downstream of the propeller that is the arc of the circle. Tests with several arc radii and several shroud lengths will be performed to determine the effects of arc radius and shroud length on the wake steering system performance. It appears from the preliminary results that, in order to get a large ratio of radial to axial thrust in the wake steering shroud system, it will be necessary to use shrouds of high divergence angles. However,

shrouds with high divergence angles tend to be less efficient in the port closed or non-steering mode, and also have some tendency to exhibit three stable states and, hence, be unreliable as steering devices. It is apparent that some compromise will have to be made in the shroud design. The optimum shroud shape must operate reliably and still produce a maximum ratio of radial to axial thrust.

The forward velocity test facility is in the process of construction and is nearly completed. A new dynamometer is being constructed similar to the one used in the static tests. Also, a shroud with an interchangeable aft section is being fabricated for use in the forward velocity tests. An analytical investigation has been conducted which indicates that the existing mathematical models cannot be used to describe shroud behavior when a control port is open and the wake is separated from the internal surface of the shroud. For this reason, continued analytical approaches to this problem will be conducted at a rather low level. Our initial work has indicated that we can expect a low probability of success from these efforts and we have, therefore, decided to concentrate on the experimental testing.

111
INTRODUCTION

A wake steering shroud concept was developed by Wozniak. The system uses a propeller inside of an accelerating or decelerating shroud with control ports located just downstream of the shroud [Fig. 1]. The ports allow water to enter the inside of the shroud from the outside. With all of the ports closed, the wake from the propeller should attach to the internal surface of the shroud as it moves downstream, completely filling the inside of the shroud. As in any accelerating nozzle, the flow is accelerated forward of the propeller and, consequently, just upstream of the propeller, high velocity fluid is available which improves the efficiency of operation of the propeller in the normal mode of operation. When a control port is opened just downstream of the propeller, separation occurs downstream of that port along the inner shroud surface causing an asymmetric pressure distribution inside the shroud and, in effect, redirecting the wake at an angle to the propeller axis in a direction opposite to the port. The net effect is that a force is exerted on the shroud and propeller system in a radial direction which can apply a steering moment to the vessel to which the system is attached. When the control port is closed, the wake must reattach to the inner surface of the shroud and will then produce no radial thrust. Wozniak demonstrated that the concept was feasible by constructing a shroud and measuring the pressure distribution inside the shroud. From this information he was able to calculate the forces on the shroud and propeller system. He was able to show from this experimental work that an asymmetric pressure distribution resulted when a port was open and so, consequently, a radial force must be exerted on the shroud. The purpose of this program has been to measure the actual forces exerted by the propeller and shroud combination and demonstrate that, indeed, a radial force does exist.

Further, by relating that radial force to shroud shape it is hoped to gain a more complete understanding of the phenomenon and thereby gain the knowledge needed to optimize the design to produce a maximum ratio of radial to axial thrust. Preliminary shroud shapes for forward velocity testing will be derived from shrouds which performed well in the static tests.

I. Experimental Results

I-1. System Description

Propeller-shroud combinations to be tested are mounted on the end of a vertical beam that serves as a dynamometer. The beam is instrumented with strain gages. See Figure 2. The gages and associated instruments allow the axial and radial horizontal forces produced by the propeller and shroud to be recorded as functions of time on an oscillograph. The moments about the propeller axis, the beam axis and the third mutually perpendicular axis can also be recorded. The beam is damped in the horizontal plane by two mechanical dampers constructed using "airpots" manufactured by Airpot Corporation to effectively provide nearly optimum dynamometer damping. The beam and shroud are immersed in a tank .914 meters by 2.44 meters with a water depth of .61 meters. The tank is baffled so as to reduce recirculation eddies in the region of the shroud which would occur due to the finite tank size and the pumping action of the propeller. Tests performed in a large pool verify that the test results in this tank are essentially equivalent to open water tests at zero forward velocity.

The propeller is driven by a DC motor through a flexible shaft at speeds of from 0 to 65 revolutions per second. Propeller torque is measured by measuring and recording armature current. Motor dynamometer tests were used to establish the relationship between armature current and propeller torque.

Pressures inside the shroud can be measured by means of a manometer bank connected to the shroud by tubing through the side of the tank.

A special shroud holder has been constructed which allows the inside shroud shape to be easily and rapidly changed. The shroud holder can be mounted on the same dynamometer used for testing the aluminum shrouds. The

system is shown in Figure 3. The shroud holder has a cylindrical inner surface of fixed diameter in the region of the control port. This ring contains the port valve assembly which is rotatable. The valve is a flapper valve located on the inner surface of the shroud. This valve is actuated by means of an air cylinder. The shroud surface fore and aft of the holder can be changed by inserts which are machined out of wax stiffened by a section of aluminum pipe. The machining of the wax is done on a lathe using heavy gauge sheet metal templates which have been cut to a prescribed shape.

It should be pointed out that the dynamometer is equipped to measure only forces in the horizontal plane. This enables the measurement of shroud axial thrust and one component of radial force. Another mutually perpendicular component is obtained by repeating the test run and opening a port located at 90° from the first port for the aluminum shrouds or rotating the port-valve assembly 90° in the case of the wax shroud holder. The two components are combined analytically to determine the radial force magnitude and direction, relative to the open port location.

Moments are measured about the three mutually perpendicular axes located at the intersection of the propeller plane and its axis. The moments can be used to exactly locate the shroud force vector. Measurements indicate that the vector is located inside the aft section of the shroud with only small variations in its location. A typical example is the data collected on Aluminum Shroud No. 2. The radial force moment arm with respect to the dynamometer moment axis was calculated to be 3.9 cm aft of the propeller plane with an average variation of $\pm 3.8\%$. The aft section of this shroud is 4.5 cm long. This would indicate that the resulting force lies within the aft section of

the shroud. This conclusion can also be reached from calculations performed using the shroud pressure measurements during open port operation or from a simplified momentum point of view. The shroud will be mounted on a submersible at distances from the submersible center of gravity which are as large as possible to get large turning moments. Hence, the errors in vessel turning moments which occur due to variations in the location of the radial thrust vector will be small. In view of this, it was decided to discontinue making moment measurements.

I-2. Dimensionless Numbers

For a given propeller and shroud design, it can be shown that

$$\text{Thrust} \equiv F = f_1(V, n, D, \rho, \mu), \text{ nt}$$

$$\text{Pressure at any point} - \text{ambient pressure} \equiv \Delta p = f_2(V, n, D, \rho, \mu), \text{ nt/m}^2$$

where

$V \equiv$ relative velocity of shroud and water, m/sec.

$n \equiv$ propeller speed, rev/sec.

$D \equiv$ propeller diameter, m

$\rho \equiv$ fluid density, Kg/m³

$\mu \equiv$ fluid viscosity, nt-sec/m²

A dimensional analysis yields

$$\frac{F}{\rho n^2 D^4} = \phi_1 \left(\frac{V}{nD}, \frac{\rho n D^2}{\mu} \right)$$

and

$$\frac{\Delta p}{\rho n^2 D^2} = \phi_2 \left(\frac{V}{nD}, \frac{\rho n D^2}{\mu} \right)$$

This is one set of dimensionless numbers, others are also possible.

In most submersible and ship designs, Reynolds number is very high so that

the flow is essentially turbulent and independent of Reynolds number. In the testing program, Reynolds Number based on tip speed = $\frac{\rho \pi n D^2}{\mu}$, varied from .75 to 3.75×10^5 at propeller speeds of 16 to 80 rev/sec. In addition, the Cavitation Number based on tip speed = $\frac{P_a - P_v}{\frac{1}{2} \rho (\pi n D)^2}$ has a minimum value of 1.63 which is large enough to insure that propeller cavitation is not occurring in the tests. Hence, the dimensionless equations can be simplified

$$\frac{F}{\rho n^2 D^4} = \phi_1 \quad \frac{V}{nD}$$

and $\frac{\Delta p}{\rho n^2 D^2} = \phi_2 \quad \frac{V}{nD}$

where $\frac{F}{\rho n^2 D^4} \equiv$ thrust coefficient K_t

$$\frac{V}{nD} \equiv \text{advance coefficient } J$$

$$\frac{\Delta p}{\rho n^2 D^2} \equiv \text{pressure coefficient } K_p$$

The primary focus of the present test program is to evaluate performance of the steering system at zero forward velocity. Hence, the advance coefficient is zero. Thus, the thrust coefficient at zero forward velocity and the pressure coefficient distribution inside the shroud characterize the performance of a given propeller and shroud geometry.

1-3. Data

The preliminary series of wax shrouds that were investigated are described quantitatively in the appendix, but they can also be described qualitatively.

Shroud No. 1 is the most radical in terms of its design, whereas, Shroud No. 7 is the most radical design. Shroud No. 1 is the least divergent. Shroud No. 7 is only slightly more divergent, but the shape of its aft section is stepped, then straight back at a fixed angle of divergence. The aft sections of shrouds Nos. 1, 2, 4 and 5 are approximately the arcs of circles - No. 3 is a hyperbola and No. 6 the canted arc of a circle. Furthermore, No. 6 is the most divergent of all the shrouds. Generally speaking, the divergence angle increases going from Shroud No. 1 to Shroud No. 6.

The investigation was divided into two parts. The first part was concerned with the measurement of the pressure distribution inside an aluminum shroud similar to wax Shroud No. 5. The second part was concerned with the measurement of the radial and axial thrust produced by the wax shrouds. All shrouds were tested using a two bladed propeller with pitch to diameter ratio equal to 1.43.

Before proceeding, it is important to recognize that the wake steering device must have two stable modes of operation depending on whether the control port is open or closed. These are as follows:

If the control port is closed:

The propeller wake must be attached to the inner surface of the shroud. This will be called State I.

If the control port is open:

The propeller wake must be separated downstream of the control port. This will be called State II.

During the tests, a third state was observed. This is the state that occurs after the port is closed. The wake remains partially separated from the shroud and does not return to State I nor remain in State II. In this state, the

pressure distribution inside the shroud was erratic. This will be called State III.

The pressure distribution was measured for a propeller and shroud in States I and II. The results are presented in Figures 4 and 5, respectively. The pressure coefficient (K_p) was plotted versus angular position with respect to the control port and axial position (z/L). The axial position of the propeller plane is located at $z/L = 0.38$. In Figure 4, it can be seen that the wake is completely attached to the walls along the full length of the shroud. This is the State I described previously. In Figure 5, it can be seen that the wake is separated behind the propeller plane, all the way to the exit plane on one side, but that it is attached on the other side (State II). The slight antisymmetrical distribution in Figure 5 is attributed to the rotational character of the fluid in the wake.

The axial and radial thrust of wax shrouds Nos. 1 to 5 were measured. The log of the thrust is plotted versus the log of the propeller speed. A straight line through the data defines a thrust coefficient. The results are presented in Figures 6 to 10. For shrouds Nos. 6 and 7, thrust could not be measured because of erratic and unsteady behavior due to wake separation (State III). The coefficient of radial thrust (K_{tr}), the coefficient of axial thrust in State I with the ports open (K_{tapo}), the coefficient of axial thrust in State II with the ports closed (K_{tapc}) and the ratio of the coefficient of radial thrust to axial thrust (K_{tr}/K_{tapo}) were computed. For the purpose of comparison, the coefficients of thrust are presented in the following table.

Table I Thrust Coefficients

Shroud No.	K_{tr}	K_{tapc}	K_{tapo}	L_{tr}/K_{tapo}
1	.117	.610	.649	.181
2	.154	.512	.558	.275
3	.231	.475	.554	.417
4	.269	.499	.610	.441
5	.308	.404	.506	.609

Note that the axial thrust coefficient with a port open is greater than the coefficient with the port closed for all the shrouds. This is due to wake separation. In shrouds Nos. 1 and 2, the values of K_{tapo} will decrease to the value of K_{tapc} when the port closes since the wake will reattach returning to State I. In shrouds Nos. 3, 4, and 5, however, the wake will not reattach when the port is closed and the wake will be in State III. Instead, the axial thrust increases. Note that the radial thrust K_{tr} and ratio of radial to axial thrust K_{tr}/K_{tapo} increases from shrouds NOs. 1 to 5 as might be expected since there is also an increase in shroud angle of divergence. However, the thrust ratio is K_{tr}/K_{tapo} and is inflated by a substantial decrease in the axial thrust coefficient, K_{tapo} from shrouds Nos. 1 to 5.

The overall results from the measurements of pressures and thrusts reveal that the series of shrouds tested can be divided into four different subsets according to their behavior and can be classified in terms of their reliability of operation.

Subset A - 2 stable states (I and II) - totally reliable

Shroud No. 1 - This shroud is totally reliable

Subset B - 2 stable states (I and II) - occasionally will go to State III - partially reliable.

Shroud No. 2 - This shroud is reliable 95% of the time.

Subset C - 3 stable states (I, II, and III) - unreliable

Shroud No. 3, 4 and 5 - These shrouds will go from State I to State II

to State III, but not backwards.

Subset D - One unstable state (I), two stable states (II and III) - unreliable

Shroud Nos. 6 and 7 - In these shrouds, the wake often separates when the control port has not been opened. These shrouds will go from state I to State II to State III, but not backwards.

II. Mathematical Model

The problem of mathematically modelling the flow field in and around a shrouded propeller is complex. Some hydrodynamic models have been obtained by earlier investigators and in spite of their sophistication, agreement with operating test results over a range of operating conditions has only been fair [1] - [7]. The usual approach in the analysis of such flows involves the use of ring vortices, or ring sources, and, assuming no separation, a solution is obtained for a preselected shape possessing axial symmetry. The object of the current research is to identify shroud geometries which will yield flow fields particularly favorable to producing lateral thrusts when operating with an open side port beyond the propeller plane. Because of the immense mathematical difficulties posed by the non-symmetric and separated nature of such a flow field, both within and around the outside of a shroud operating in this mode a useful hydrodynamic model, has been ruled out. Instead, the results of existing analyses of rotating flows possessing axial symmetry have been used to guide the iteration process for the experimental part of this investigation.

The work of Fraenkel [8] and Clow [9] have been used to qualitatively characterize the nature of the flow field beyond the propeller plane. Those investigations, dealing with rotating flows in tubes of varying cross section identify a quantity $\frac{W}{2Rw}$, the reciprocal of what is generally referred to as

the Rossby number R_o^{-1} . When R_o^{-1} is less than j_1 , the first zero of the Bessel function, J_1 , the flow is somewhat similar to that without rotation, but with modifications which have been experimentally verified in our tests. For R_o^{-1} greater than j_1 wave motions are established in the downstream flow. In our case W is the fluid axial velocity (in this case an average value) based on the shroud through flow and Rw represents the tangential velocity of the fluid at the shroud wall. As such R_o^{-1} is equivalent to twice the ratio of tangential to axial velocity or could even be regarded as a flow coefficient.

Experiments run with several propeller-shroud combinations for the purpose of determining angles of the flow in the shroud beyond the propeller plane indicate low values of swirl. The value of R_o^{-1} based upon these measurements varies from about 0.5 to 1.5, but is below j_1 which is 3.83171. Fraenkel predicted flow acceleration along the wall in an expanding flow with accompanying retardation along the axis. The greater the ratio of exit to throat areas, the more severe the effect. The shrouds tested to date have displayed this flow pattern as slowing of the flow and in some cases, reversal has been detected along the axis just outside the exit plane. The significant point in terms of the wake steering device is that flow along the wall does accelerate with rotation in the flow and this does help to overcome separation as the shroud wall angles increase toward the exit plane.

All of the shrouds tested to date, except No. 1, have displayed either a steady or fluctuating separation pattern in the exit flow producing an uncontrollable component of radial force. Because the wake separates from the increasingly divergent curved wall at some point before the exit plane, a potential flow analysis is inappropriate as a reliable model of the outlet

flow. All analyses to date [1] - [10] are based upon nonseparated flow within the shroud and are inappropriate for the separated flows encountered in the more highly divergent wake steering shrouds. The analyses of Fraenkel, Chow and others dealing with the basic characteristics of swirling duct flows are useful to the extent that they predict some of the characteristics of the flow up to the point of separation and then the core jet beyond that point in a qualitative sense.

IV. Conclusions

The test results from this preliminary series of shrouds is difficult to interpret in view of the fact that in an attempt to rapidly determine an optimum shroud shape, too many parameters such as length, divergence angle and generating shape were varied tending to mask the effects of any one parameter. It is however, apparent that to develop high radial to axial thrust ratios, the shroud must have a large angle of divergence. This requirement conflicts with the demands of low divergence angle in order to avoid unwanted separation, i.e. separation when the control ports are closed. While the widely recognized shape, 19a, of Van Manen and Oosterveld [10] may demonstrate good performance characteristics as a basic thrusting device, it will not function well as a steering device because of its low divergence angle. Clearly, a trade off between the two conflicting exit angle requirements of small angle for no separation and large angle for useful deflection of flow in the steering mode must be made.

Another important concept to emerge is that of reliability. To be reliable, a shroud must develop a radial force with a control port open. This force must disappear when the port is closed and the wake must completely reattach to the shroud surface. To determine a shroud shape or set of shroud shapes which reliably develop high radial to axial thrust ratios will require a step by

step investigation of the parameters involved. Also, the tests must be conducted at forward velocity conditions in addition to the static case.

V. Future Program

A series of static tests is planned to determine the effects of shroud divergence angle, shroud length, propeller pitch to diameter ratio and generating shape on shroud performance. The first series of shrouds to be tested will use the same shroud fore-section as Shrouds Nos. 1, 2, 3, 4, 6 and 7. The inside surface of the shroud aft section is generated by the arc of a circle. The aft section will be kept a constant length and the divergence angle varied by varying the radius of the arc. In the second series of shrouds, the inner surface will be an arc of fixed radius except they will be cut to various different lengths. In the third series, generating shapes other than the arc of a circle will be used. Time permitting, investigations of the effect of port flow on shroud switching characteristics and shroud switching capability for reversed flow will be investigated.

Construction of a forward velocity test tunnel and dynamometer have been initiated and should be completed by the end of April. The system will be capable of measuring radial and axial thrusts at advance ratios of up to 1.0. Once completed, our highest priority will be given to the forward velocity tests. Static testing will continue since, except for a recording oscillograph, both systems are essentially independent.

A method is being developed for making forward velocity shrouds in which the inside and outside shapes can be varied rapidly and economically. A shroud has been constructed using a contoured aluminum front section to

which is fastened an aft section made out of a polyester - magnesium silicate compound. Besides being economical and not too difficult to manufacture, this shroud has the additional advantage over the nozzle holder in that the ports can be located anywhere on the aft section of the shroud. This additional flexibility will enable some radical changes in shroud shape and control port design. Some preliminary static testing of nozzles whose port configuration departs from previous designs is planned.

Investigation of mathematical models of the flow for predicting pressure and separation will continue at a very low level. Two possible approaches to modelling the shroud remain to be evaluated. The first approach is to re-program an analysis by Weetman [11] for our computer. This program may give accurate shroud pressure distributions for highly divergent shrouds since it is not based on linearized assumptions. If the program is successful in predicting measured pressures, then, if possible, it will be modified for use in predicting where separation occurs.

The second approach is to utilize Chow's solution as a first order approximation to the integral equation form of the defining flow relations. It may be possible to use the zeroth order solution at each axial station, set the eigenvalue to fit the boundary conditions at the wall, and obtain a solution to the entire flow field in this manner. This approach has the advantage that it gives the velocities in the entire flow field as well as the pressures.

REFERENCES

1. Morgan, William B., Caster, E. B., "Comparison of Theory and Experiment on Ducted Propellers," 7th Symposium Naval Hydrodynamics, August, 1968.
2. Morgan, W. B., "A Theory of the Ducted Propeller With a Finite Number of Blades," University of California, Institute of Engineering Research, Berkeley, May, 1961.
3. Greenberg, M. D., Ordway, D. E., "The Ducted Propeller in Static and Low-Speed Flight," THERM, Incorporated, TAR-TR 6407, October, 1964.
4. Chaplin, H. R., "A Method for Numerical Calculation of Slipstream Contraction of a Shrouded Impulse Disc in the Static Case with Application to Other Axisymmetric Potential Flow Problems," David Taylor Model Basin Report 1857, June, 1964.
5. Ordway, D. E., Slayter, M. M., Sonnerup, B. O. U., "Three-Dimensional Theory of Ducted Propellers," THERM, Incorporated, TAR-TR 602, August, 1960.
6. Oosterveld, M. W. C., "Wake Adopted Ducted Propellers," Netherlands Ship Model Basin Publication No. 345.
7. Morgan, William B., "Some Results from the Inverse Problem of the Annular Airfoil and Ducted Propeller," Journal of Ship Research, Vol 13, No. 1, 1969.
8. Fraenkel, L. E., "On the Flow of Rotating Fluid Past Bodies in a Pipe," Proc. Roy. Soc., 1956, pp. 506-518.
9. Chow, Chuen-Yen, "Swirling Flow in Tubes of Non-uniform Cross-sections," J. Fluid Mech., Vol. 38, 1969, pp. 843-854.
10. Van Manen, J. D., Oosterveld, M. W. C., "Analysis of Ducted Propeller Design," Society of Naval Architects and Marine Engineers Annual Meeting, November, 1966.
11. R. Weetman, "Calculation of Inlet Flows by Means of a Closed Vorticity Distribution Applied to Ducted Propellers," Ph.D. Thesis, Univ. Mass., 1972.

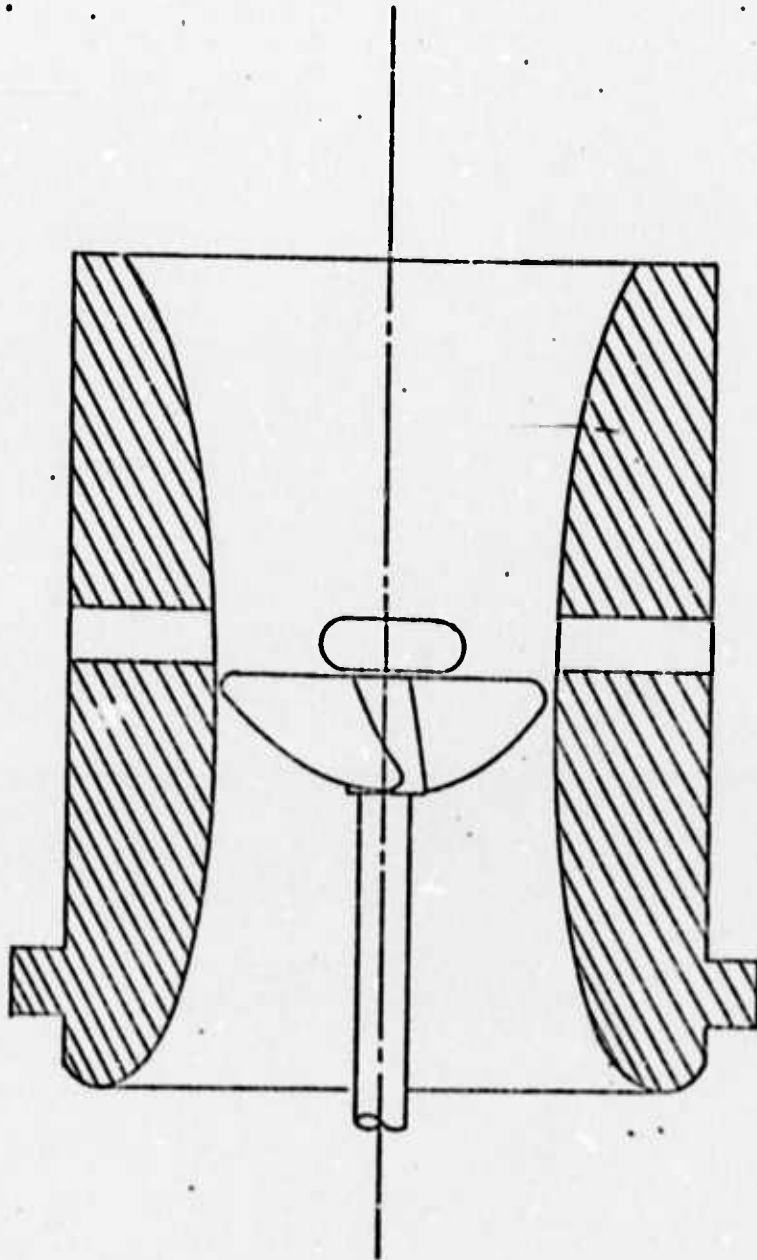


FIG.1. WAKE STEERING SHROUD DESIGN

No.2.

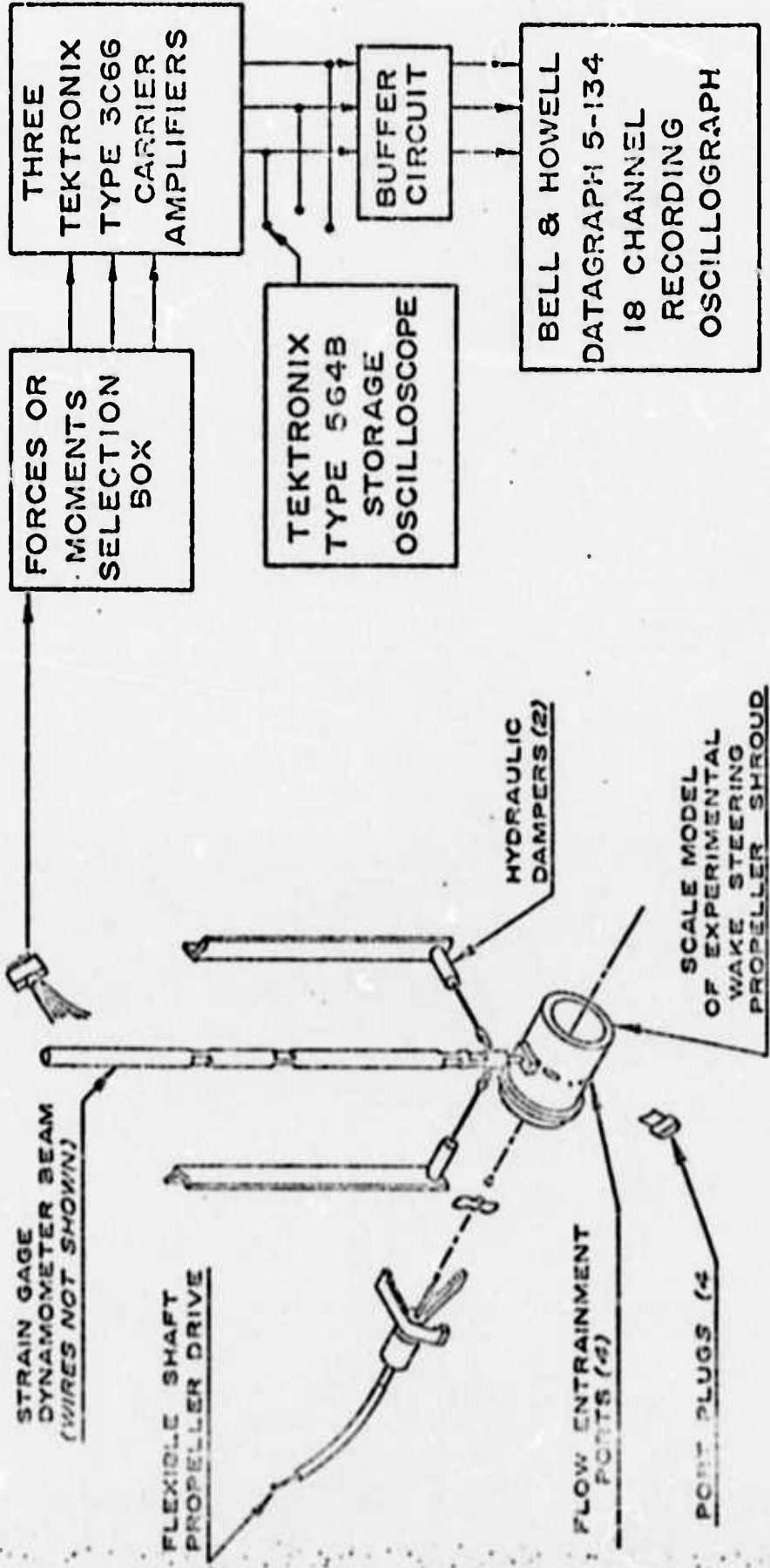


FIG. 2. SHROUD MODEL AND DYNAMOMETER

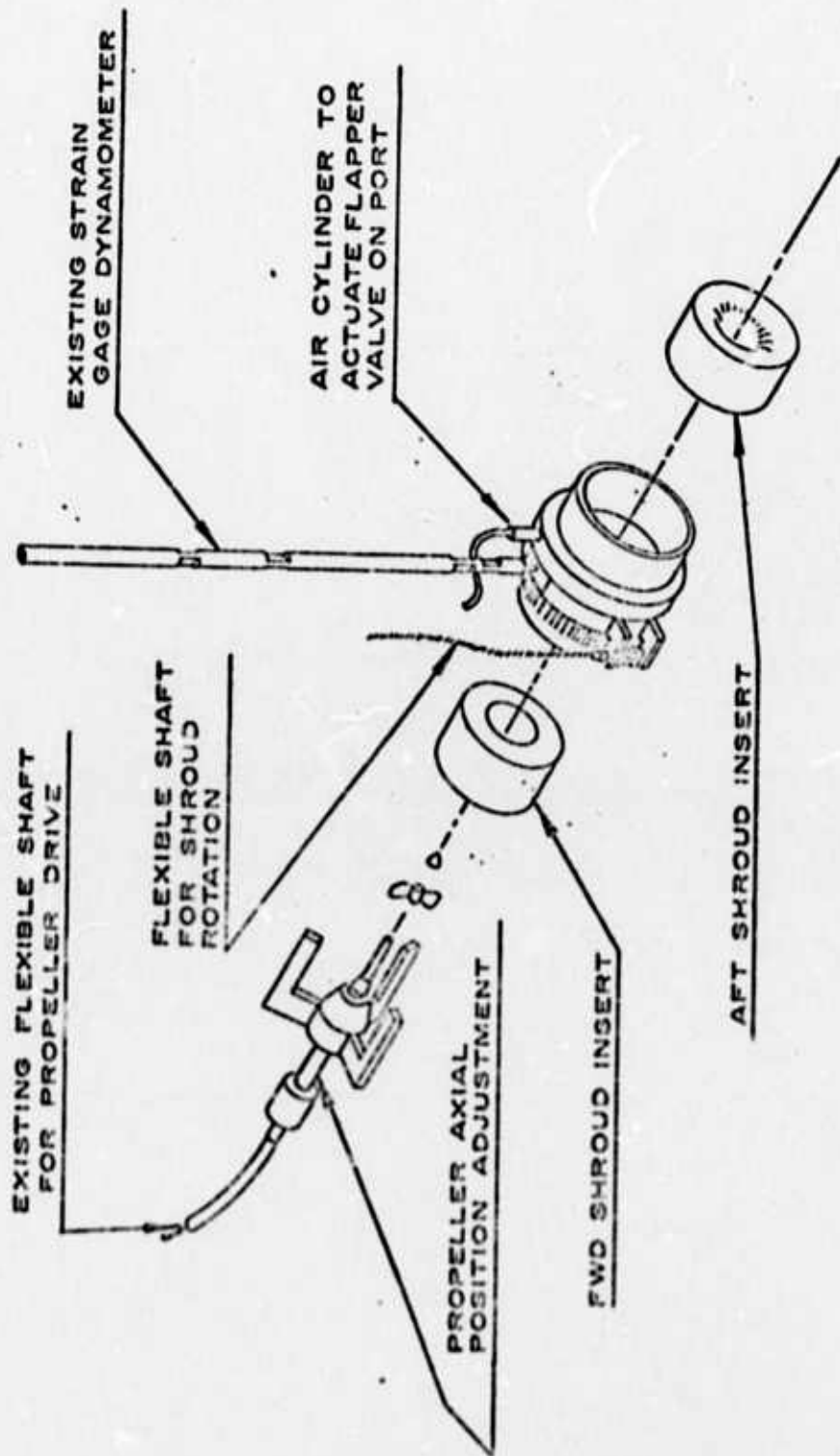


FIG.3 PROPOSED SHROUD VARIATION SYSTEM

**Best
Available
Copy**

X 32.5
O 42.5
Δ 52.5

Reproduced from best available copy.

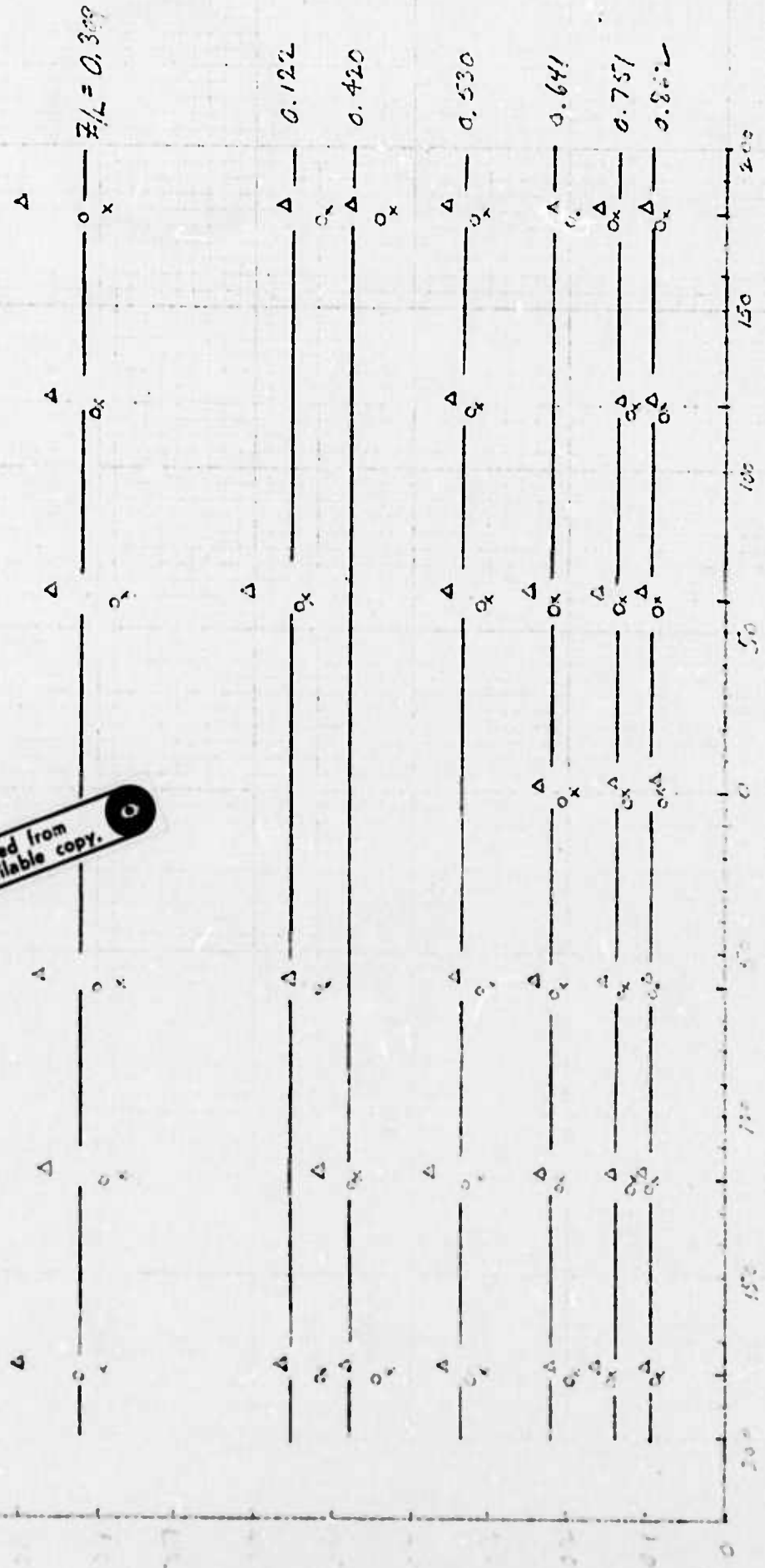


FIG. 4. PRESSURE DISTRIBUTION INSIDE ALUMINUM PROPELLER SHAFT NO. 1, WITH POLE CLOSED

Reproduced from
best available copy.

X 52.5 R/S
O 47.5 R/S
L 62.5 R/S

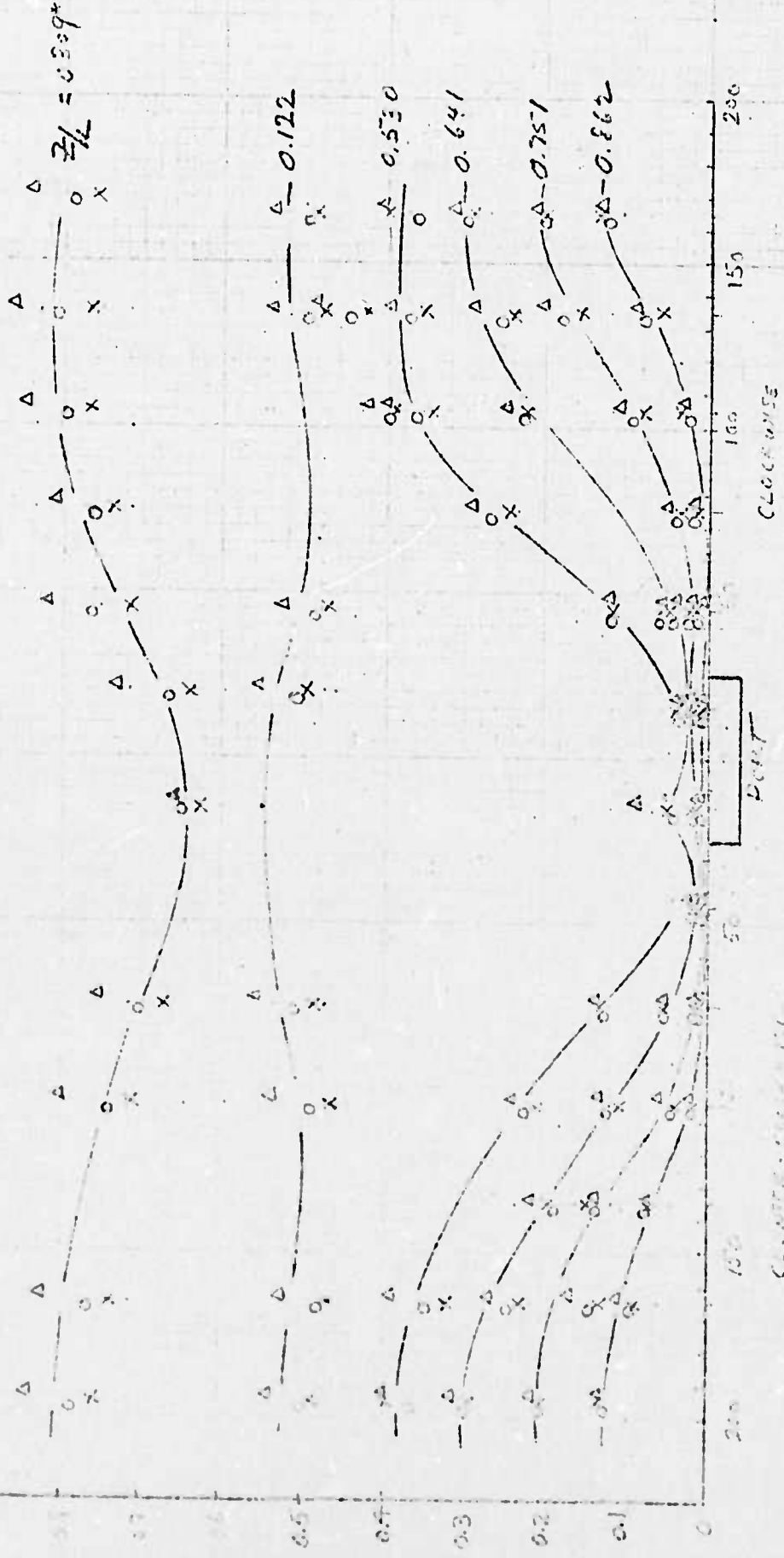
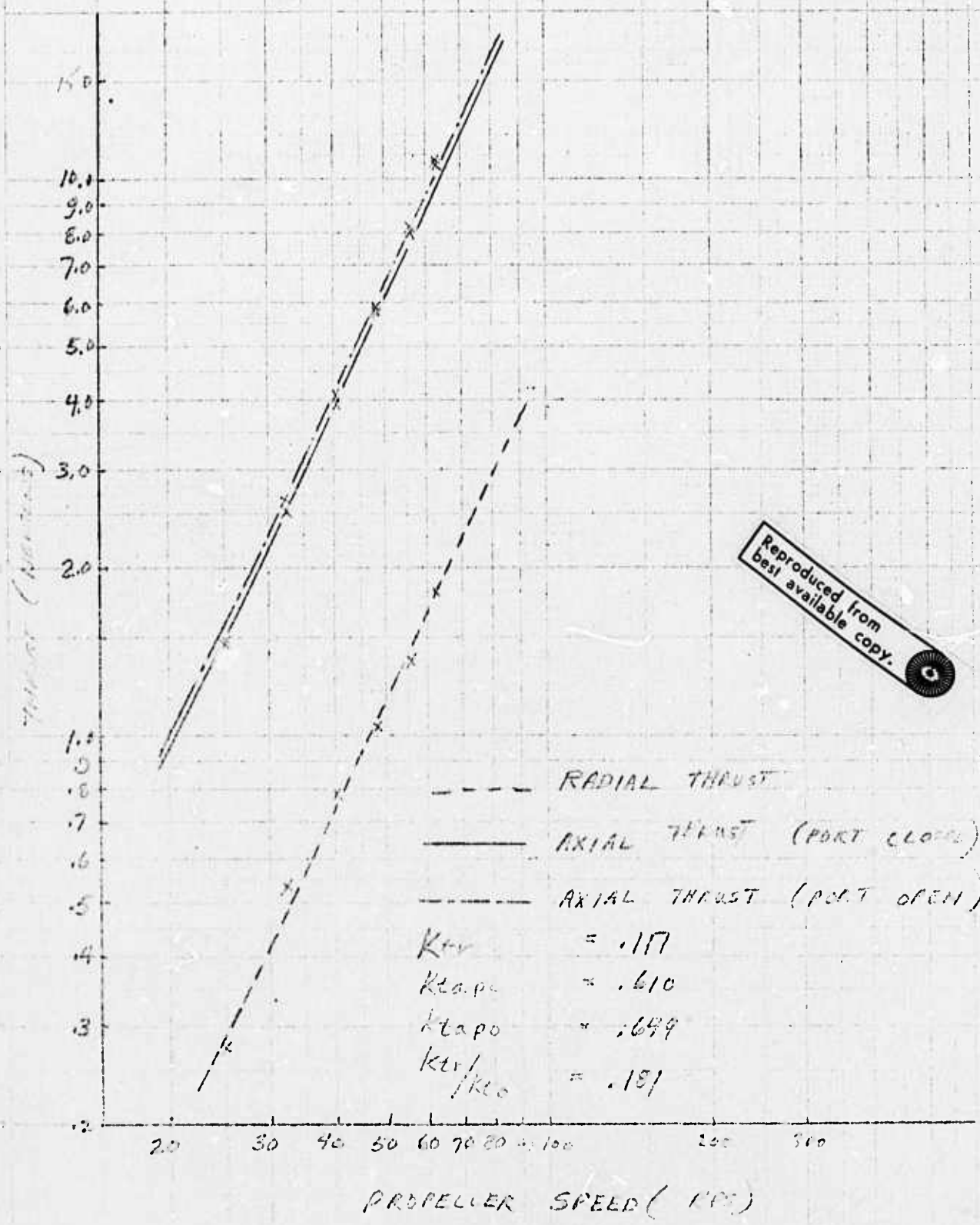
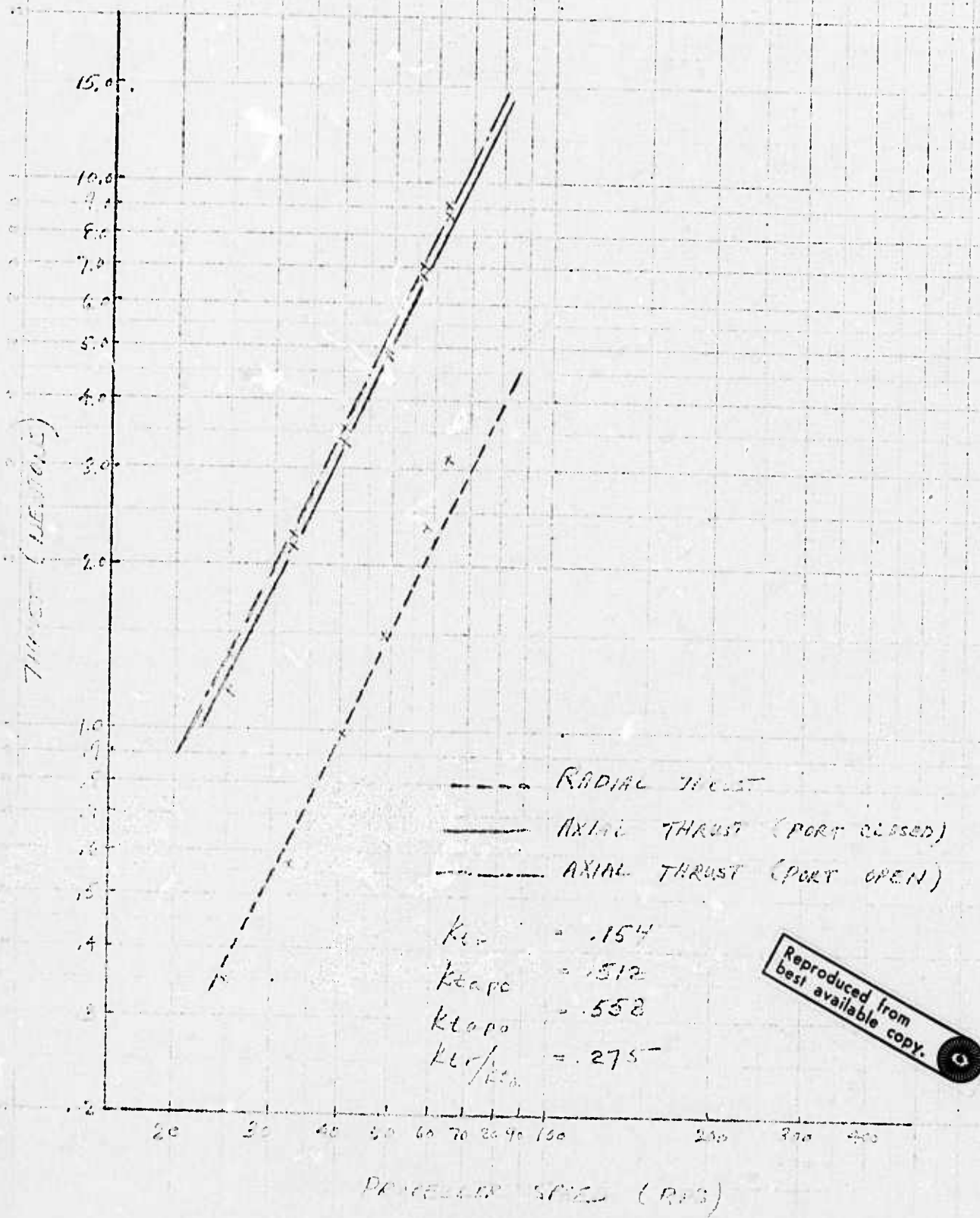


FIG. 5. PRESSURE DISTRIBUTION INSIDE ALUMINUM PROPELLER SHROUD NO. 1
ANGLE POSITION DEGREE
WITH PORT OPEN



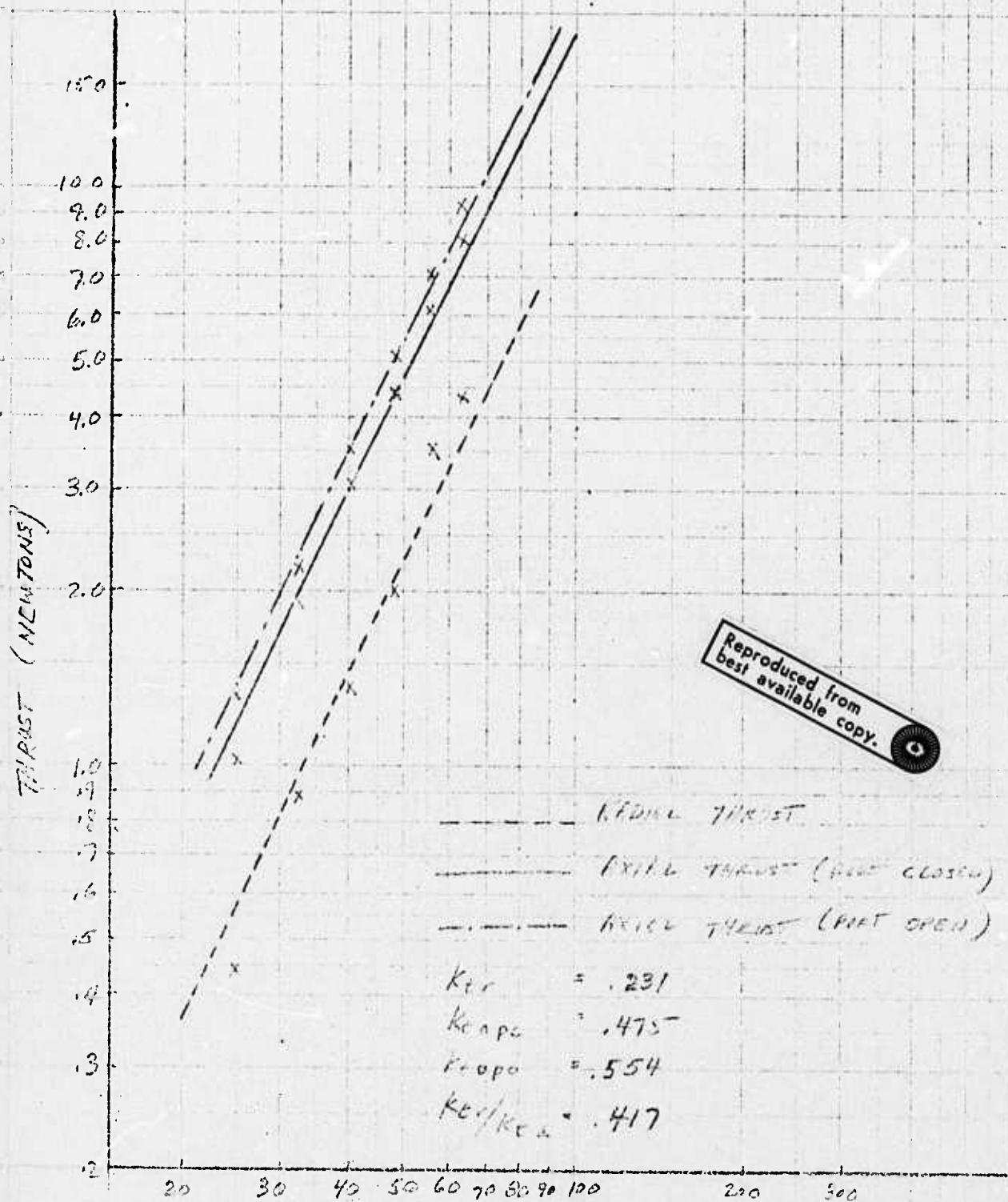
Reproduced from best available copy.

FIG. 6. AXIAL & RADIAL THRUST VS PROPELLER SPEED FOR WAK SHAGROD NO. 1



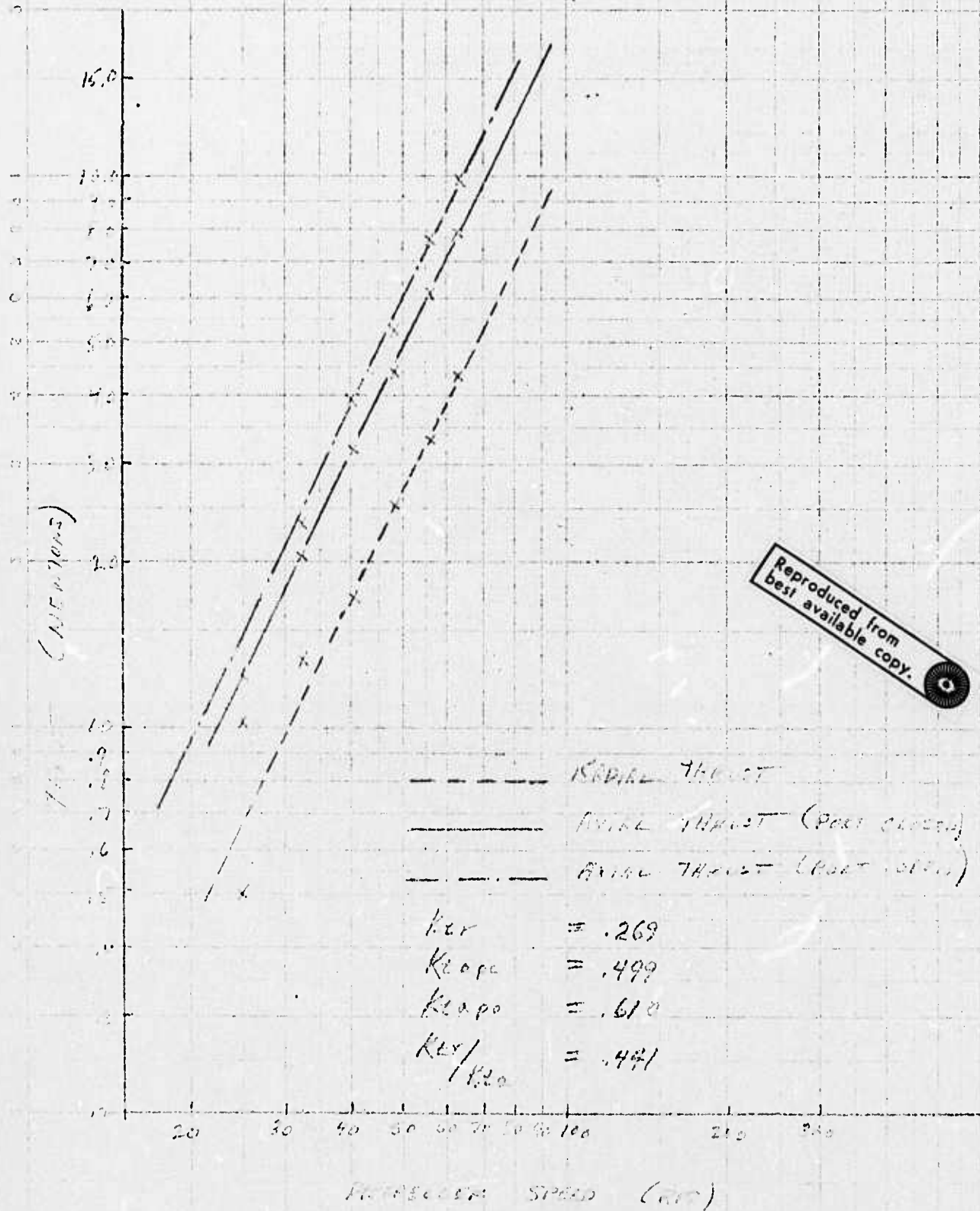
Reproduced from best available copy.

Fig. 7. Axial & Radial Thrust vs. Prop. Sp. Speed
 For W-15 Speed No. 2



PROPPELLER SPEED (RPM)

FIG. 8. WINDMILL & ENGINE THRUST vs. PROPPELLER SPEED FOR WINDMILL No. 3.



9. Axial & Radial Thrust vs Propeller Speed for Prop No. 4.

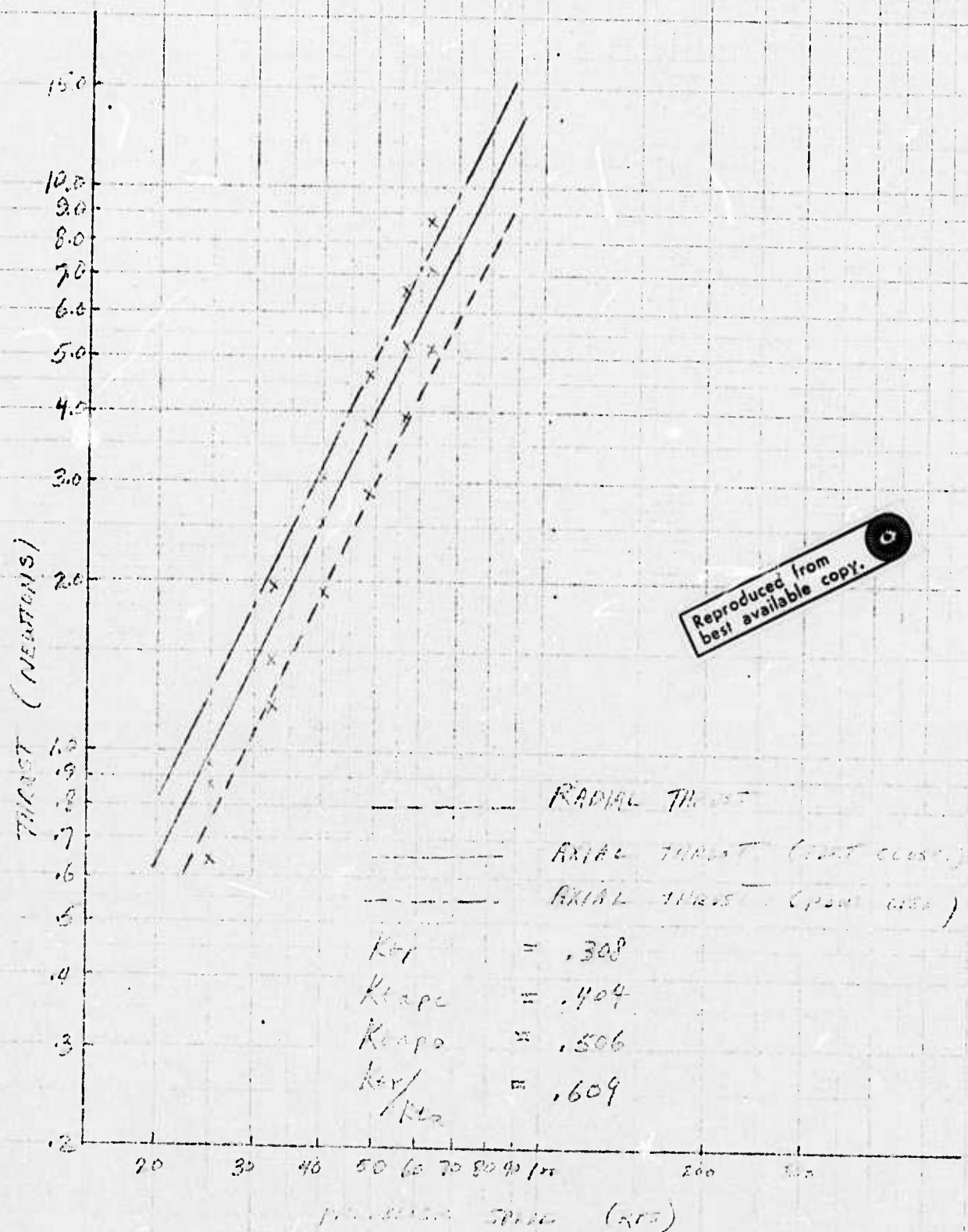
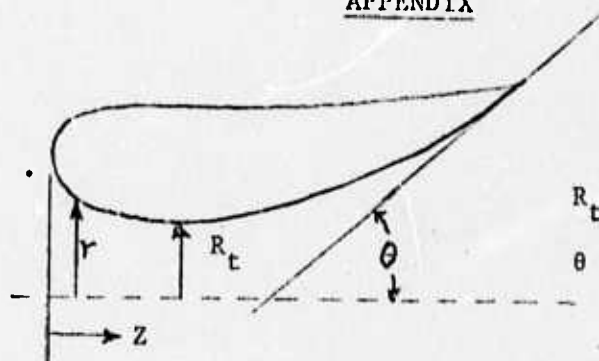


FIG 10. Thrust vs. Rotational Speed - 05, 100% Case
 For 100% Case No. 5.

APPENDIX



R_t = Radius at the throat

θ = Divergence angle

Shroud #1

$L = 11.1\text{cm}, \theta = 16.1^\circ$

Z(cm)	$r - R_t$ (cm)
0	1.42
.10	1.04
.25	.89
.51	.71
.76	.61
1.02	.51
1.37	.41
1.68	.33
1.98	.25
2.28	.21
2.64	.17
2.95	.13
3.56	.08
4.06	.05
5.08	0
↓	↓
6.53	0
7.04	.01
7.57	.06
8.05	.11
8.56	.18
9.07	.25
9.58	.35
10.08	.46
10.59	.58
11.10	.72

Shroud #2

$L = 10.5\text{cm}, \theta = 26.0^\circ$

Z	$r - R_t$
0	Same as Shroud #1
↓	↓
6.02	
6.53	.03
7.04	.08
7.57	.17
8.05	.28
8.56	.41
9.07	.57
9.58	.74
10.08	.94
10.50	1.19

Shroud #3

$L = 10.95\text{cm}, \theta = 25.0^\circ$

Z	$r - R_t$
0	Same as Shroud #1
↓	↓
6.02	
6.34	.02
6.66	.06
6.98	.13
7.29	.23
7.61	.32
7.93	.42
8.25	.54
8.56	.66
8.88	.78
9.20	.91
9.52	1.04
9.83	1.16
10.15	1.30
10.46	1.43
10.95	1.64

25.
APPENDIX

Shroud #4

$L = 10.5\text{cm}, \theta = 35.0^\circ$

Z	$r - R_t$
0	Same as Shroud #1
↓	
6.02	
6.53	.02
7.04	.07
7.57	.16
8.05	.29
8.56	.44
9.07	.64
9.58	.88
10.08	1.18
10.50	1.43

Shroud #5

$L = 10.1\text{cm}, \theta = 33.0^\circ$

Z	$r - R_t$
0	1.73
.10	1.04
.20	.80
.30	.68
.40	.59
.50	.51
.70	.42
.90	.33
1.10	.29
1.30	.23
1.50	.19
1.70	.16
2.00	.11
2.30	.04
2.70	.02
3.10	0
3.60	0
4.05	0
4.55	.03
5.05	.09
5.45	.14
5.85	.21
6.15	.29
6.45	.38
6.75	.47
7.05	.57
7.35	.66
7.65	.77
7.95	.88
8.25	1.00
8.55	1.15
8.85	1.30
9.15	1.48
9.45	1.63
0.75	1.83
10.10	2.05

Shroud #6

$L = 10.5\text{cm}, \theta = 37.0^\circ$

Z	$r - R_t$
0	Same as Shroud #1
↓	
6.02	
6.52	.05
6.52	.10
7.32	.17
7.72	.26
8.12	.37
8.52	.51
8.92	.68
9.32	.81
9.72	1.10
10.12	1.33
10.50	1.60

Shroud #7

$L = 10.5\text{cm}, \theta = 18.0^\circ$

Z	$r - R_t$
0	Same as Shroud #1
↓	
6.02	
6.12	.03
6.22	.11
6.32	.23
6.42	.36
6.52	.40
6.72	.46
7.02	.55
7.52	.69
8.02	.73
9.02	1.08
10.50	1.52